Many-body Chern insulator in the Kondo lattice model on a triangular lattice

Kota Ido and Takahiro Misawa

Institute for Solid State Physics, University of Tokyo, 5-1-5 Kashiwanoha, Kashiwa, Chiba 277-8581, Japan

The realization of topological insulators induced by correlation effects is one of the main issues of modern condensed matter physics. An intriguing example of correlated topological insulators is a magnetic Chern insulator induced by a noncoplanar multiple-Q magnetic order. Although the realization of the magnetic Chern insulator has been studied in the classical limit of the Kondo lattice model, research on the magnetic Chern insulator in the original Kondo lattice model is limited. Here, we investigate the possibility of the many-body Chern insulator with the noncoplanar triple-Q magnetic order in the Kondo lattice model on a triangular lattice. Using the many-variable variational Monte Carlo method, we reveal that the triple-Q magnetic order becomes a ground state at quarter filling in an intermediate Kondo coupling region. We also show that the many-body Chern number is quantized to one in the triple-Q magnetic ordered phase utilizing the polarization operators. Our results provide a pathway for the realization of the many-body Chern insulator in correlated electron systems.

I. INTRODUCTION

The Kondo coupling [1]—magnetic interaction between localized spins and conduction electrons—has been extensively studied as a driving force for inducing several exotic quantum phases originally in heavy-fermion systems [2–6]. The Kondo coupling leads to two main effects: the long-range Ruderman-Kittel-Kasuya-Yosida (RKKY) interactions between the localized spins [7–9], and the formation of a singlet between the local spins and the conduction electrons. The competition between these two effects gives rise to a quantum critical point at which the magnetic transition temperatures become zero [10]. The study of spillover effects emergent from the quantum critical points, such as non-Fermi liquid behaviors and unconventional superconductivity, has been one of the main topics in condensed matter physics [3–6].

Moreover, the Kondo coupling has been also found to manifest various quantum phases, such as a ferromagnetic phase via the double-exchange interaction [11–13], a charge-ordered phase [14–16], a partial disordered phase [17,18], topological orders [19], exotic superconductivity [20,21] including topological superconductivity [22–24], and a skyrmion crystal with a multiple-Q magnetic order [25–29]. In particular, the emergence of a noncoplanar triple-Q magnetic ordering has attracted significant interest since it can be regarded as the magnetic topological insulators, i.e., the magnetic Chern insulators [30–32], which show the quantum Hall effects without magnetic fields [33–35]. However, previous theoretical studies were primarily conducted for the classical limit of the Kondo lattice models that ignore quantum effects. The quantum effects were only discussed within the linear spin-wave approximation to the ferromagnetic Kondo lattice model [36].

To clarify the topological nature of the triple-Q magnetic ordered state, direct calculation of the many-body Chern number is necessary. For noninteracting systems, efficient methods for calculating the Chern number [37,38] have been proposed and applied to a wide range of systems. However, these

methods cannot be applied to interacting systems where wave number is not a good quantum number. A pioneering work by Niu *et al*. [39] shows that the many-body Chern number can be calculated by regarding the twisted boundary condition as an effective wave number. However, the numerical cost is huge in this approach, since it requires integration over all twisted boundary conditions. Recently, several efficient methods that do not require full integration have been proposed [40–43]. Despite this theoretical progress, it remains a significant challenge to develop an efficient and flexible numerical method that can calculate the many-body Chern number in a wide range of interacting systems with large system sizes.

In this paper, we examine the stability of the triple-Q magnetic ordered phase in a quantum spin 1/2 Kondo lattice model on a triangular lattice by using the many-variable variational Monte Carlo (mVMC) method [44–47], which can take into account both spatial correlations and quantum fluctuations efficiently. Our results demonstrate that the triple-Q state is indeed realized in an intermediate Kondo coupling region at quarter filling. Furthermore, we show that the triple-Q state has the nontrivial Chern number by explicitly calculating the many-body Chern number based on Resta's polarization operator [42,43,48]. Our findings provide a theoretical basis for understanding the emergence of magnetic topological insulators induced by the Kondo coupling.

II. MODEL AND METHOD

The Kondo lattice model on a triangular lattice shown in Fig. 1(a) is defined by

$$\mathcal{H} = -\sum_{i,j,\sigma} t_{i,j} c^{\dagger}_{i\sigma c} c_{j\sigma c} + J \sum_i \boldsymbol{S}^c_i \cdot \boldsymbol{S}^s_i, \tag{1}$$

where $c^{\dagger}_{i\sigma c}$ and $c_{i\sigma c}$ are the creation and annihilation operators of electrons with spin σ at the ith site on the conduction layer, respectively. $\boldsymbol{S}^{c/s}_i$ denotes the spin 1/2 operator at the
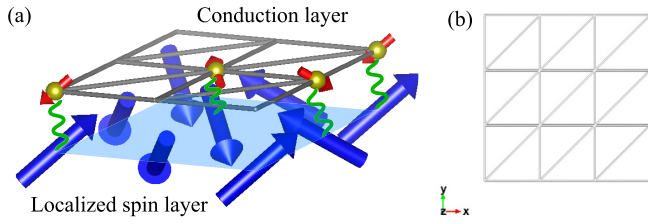
245114-1

FIG. 1. (a) Schematic figure of the Kondo lattice model on the triangular lattice. Top and bottom layers represents conduction and localized spin layers, respectively. (b) Square lattice with next-nearest hoppings deformed from the triangular lattice.

*i*th site on the conduction(*c*)/localized spin(*s*) layer, namely, $S_i^{\lambda,\alpha} = \sum_{\sigma,\sigma'} c_{i\sigma\lambda}^\dagger \sigma_{\sigma,\sigma'}^\alpha c_{i\sigma'\lambda}/2$ where σ^α is the Pauli matrix for $\alpha = x, y, z$. We set $t_{ij} = t$ for the nearest-neighbor sites on the lattice and $t_{ij} = 0$ for the others. We focus on the antiferromagnetic Kondo lattice system, namely, $J > 0$. As shown in Fig. 1(b), we map the triangular lattice onto the square lattice with next-nearest hoppings. Both the conducting electron and the localized spin layer have $N_s = L \times L$ sites under the periodic-periodic boundary condition.

To analyze the Kondo lattice model on a triangular lattice at quarter filling, we employed the mVMC method, which enables us to obtain the accurate wave functions of ground states in strongly correlated electron systems [44–47]. As a trial wave function for the VMC method, we adopted the generalized pair product wave function with the Gutzwiller-Jastrow correlation factors, which are given as

$$|\psi\rangle = \mathcal{P}_G \mathcal{P}_J |\phi\rangle, \tag{2}$$

$$|\phi\rangle = \left(\sum_{I,J} f_{IJ} c_I^\dagger c_J^\dagger \right)^{N/2} |0\rangle, \tag{3}$$

$$\mathcal{P}_G = \exp\left(-\sum_{\lambda=c,s} g^\lambda \sum_i n_{i\uparrow\lambda} n_{i\downarrow\lambda} \right), \tag{4}$$

$$\mathcal{P}_J = \exp\left(-\sum_{i,j} v_{ij}^c (n_{ic} - 1)(n_{jc} - 1) \right), \tag{5}$$

where $n_{i\sigma\lambda} = c_{i\sigma\lambda}^\dagger c_{i\sigma\lambda}$, $n_{i\lambda} = \sum_\sigma n_{i\sigma\lambda}$, and N is the total number of electrons and localized spins. Indices I and J include site, spin and layer indices, i.e., $I = (i, \sigma_i, \lambda_i)$ and $J = (j, \sigma_j, \lambda_j)$. We treat g^c, v_{ij}^c and f_{IJ} as the variational parameters. We fix g^s to infinity to exclude the double occupation on the localized spin layer. We use the stochastic reconfiguration method to simultaneously optimize all the variational parameters [49].

In this study, we consider four magnetic-ordered states as candidates of the ground states, i.e., the triple-*Q* magnetic ordered state, the double-*Q* magnetic ordered state, the stripe magnetic ordered state, and the ferromagnetic state. Schematic pictures of these ordered states are shown in Fig. 2(a). To obtain the triple-*Q* state and ferromagnetic state, the generalized pairings f_{IJ} are treated as the complex numbers. For the other states, we only optimize the real part of f_{IJ}. We note that g^c and v_{ij}^c are treated as the real numbers.
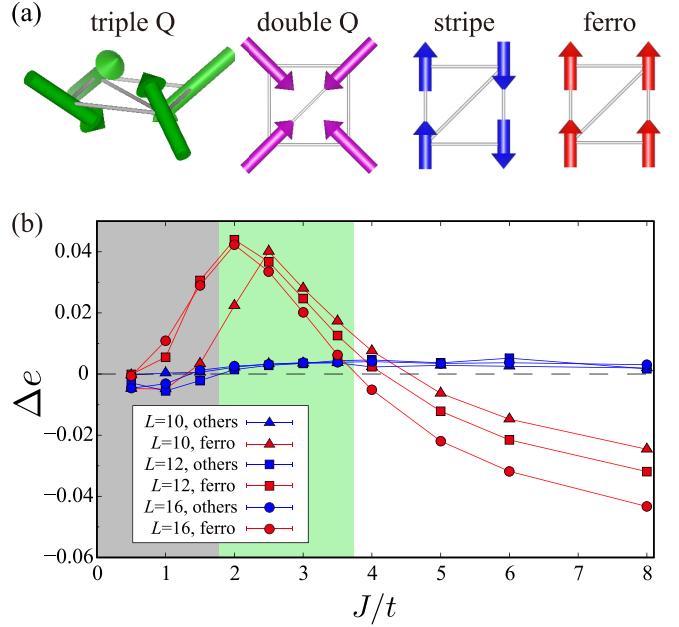

FIG. 2. (a) Spin configuration considered as initial states for the mVMC calculations. (b) *J* dependence of the energy measured from the triple-*Q* state, $\Delta e = (E - E_{\text{triple}-Q})/N_s$. Red symbols denote the results for the ferromagnetic state. Blue symbols represent the energy difference between the energy of the triple-*Q* state and the lowest energy among the other magnetic states such as double-*Q* and stripe states.

We impose the 1×1 and 2×2 sublattice structures on f_{IJ} to efficiently represent the ferromagnetic state and the other magnetic states, respectively. We also assume that v_{ij}^c has the translational symmetry reflecting the lattice structure to reduce the numerical costs.

III. RESULTS

A. Ground-state phase diagram

We examine the possibility of the triple-*Q* state in the Kondo lattice model defined in Eq. (1). Figure 2(b) shows *J* dependence of the energy measured from the triple-*Q* state for $L = 10$, 12, and 16. We find that the triple-*Q* state becomes the ground state for $2 \leqslant J/t \leqslant 3.5$. We note that the triple-*Q* state and the ferromagnetic state can always stabilize while the optimization of the double-*Q* and stripe states tends to be unstable and they sometimes converge to other magnetic states such as the ferromagnetic state. Thus, in Fig. 2, we use *others* to describe the magnetically ordered states other than the triple-*Q* state and the ferromagnetic state.

For $J/t < 2$, because of the severe competition among the magnetic-ordered states, we cannot identify the ground states clearly within available system sizes. In this weak coupling region, the long-period magnetic ordered state may be realized. To examine the possibility of the long-period magnetic ordered phases, it is necessary to extend the sublattice structure of the variational parameters. Since the numerical cost for larger sublattice structures is very high, we leave this issue for a future study. In the strong coupling region ($J/t > 3.5$), we find that the ferromagnetic ordered phase becomes the
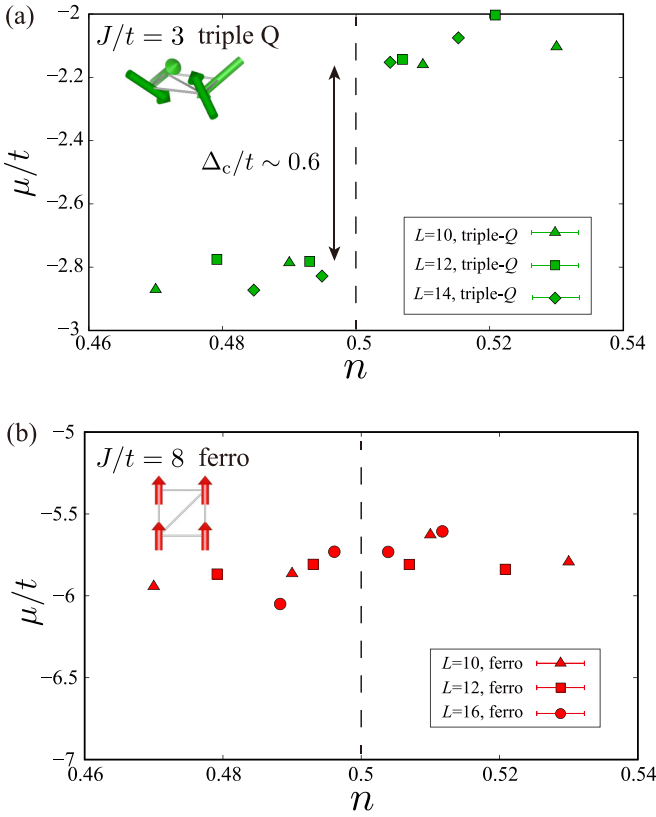
FIG. 3. Doping dependence of the chemical potential μ of (a) the triple-Q state for $J/t = 3$ and (b) the ferromagnetic state for $J/t = 8$.

ground state. This is consistent with the previous studies in the classical limit [28].

Next, to clarify whether the obtained triple-Q state is insulating or not, we calculate the chemical potential μ as a function of the electron density $n = N_e/N_s$, which is defined as $\mu(N_e + 1) = (E(N_e + 2) - E(N_e))/2$, where $E(N_e)$ denotes the total energy with the number of electrons N_e. Figure 3(a) shows μ-n plot of the triple-Q state for $J/t = 3$. From this plot, we evaluate the charge gap as $\Delta_c/t \sim 0.6$. This is quite large compared with the gap arising from the spin-orbit interaction, which is a driving force to open the charge gap in conventional topological insulators. Note that, as shown in Fig. 3(b), the ferromagnetic state does not have a finite charge gap and thus is metallic.

Here, we examine magnetic properties of the ground states. We calculate the Fourier-transformed magnetic moment $M_\alpha^\lambda(\boldsymbol{q}) = \frac{1}{N_s} \sum_i \langle S_i^{\lambda,\alpha} \rangle e^{-i\boldsymbol{q} \cdot \boldsymbol{r}_{i\lambda}}$, where $\boldsymbol{r}_{i\lambda} = (x_{i\lambda}, y_{i\lambda})$ is the position vector at the ith site on λ layer. Figure 4 shows $M_\alpha^\lambda(\boldsymbol{q})$ of the ground states. To enhance the visibility, we plot $4M_\alpha^c(\boldsymbol{Q})$ and $-M_\alpha^s(\boldsymbol{Q})$. Note that $M_\alpha^s(\boldsymbol{Q})$ has the opposite sign of $M_\alpha^c(\boldsymbol{Q})$ since we consider the antiferromagnetic Kondo coupling.

Figure 4(a) shows the size dependence of $M_\alpha^\lambda(\boldsymbol{Q})$ for $J/t = 3$, where $\boldsymbol{Q}$ represents an ordering wave vector. We also plot the $|M_\alpha^s(\boldsymbol{q})|$ in the momentum space for $L = 16$ in the inset of Fig. 4(a). We see that $M_\alpha^s(\boldsymbol{q})$ has sharp Bragg peaks for each α, which signal long-range magnetic order at three different $\boldsymbol{Q}$s. We find that $\boldsymbol{Q}$s are $(\pi, 0)$, $(0, \pi)$ and (π, π) for $\alpha = x, y$ and z, respectively. As shown in Fig. 4(a), size dependence of
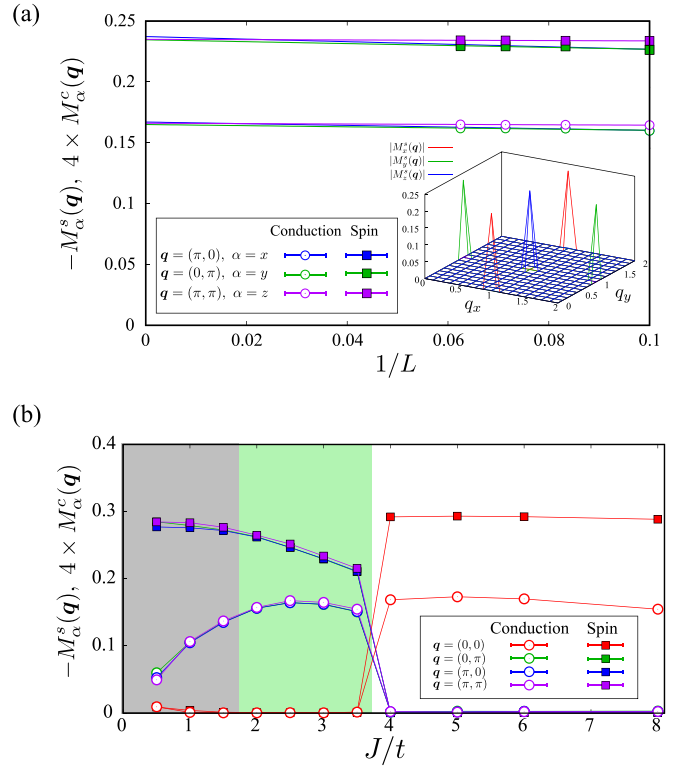

FIG. 4. Magnetic properties of the triple-Q state and the ferromagnetic state in the triangular Kondo lattice model. (a) Size dependence of $M_\alpha^\lambda(\boldsymbol{q})$ of the ground state for $J/t = 3$. Circles and squares represent the results for the magnetic moments $M_\alpha^c(\boldsymbol{q})$ and $M_\alpha^s(\boldsymbol{q})$, respectively. Colors of the symbols denote the wave number $\boldsymbol{q}$ and the direction of the spin operator α. Thin lines shows the linear lines fitted from $M_\alpha^\lambda(\boldsymbol{q})$ for each $\boldsymbol{q}$, α and λ. Inset shows the $\boldsymbol{q}$ dependence of the magnetic moment on the localized spin layer $|M_\alpha^s(\boldsymbol{q})|$ for $J/t = 3$. Red, green, and blue lines denote x, y, and z components of the magnetic moment, respectively. (b) J dependence of magnetic order parameters for $L = 16$. Squares and circles represent the results of spin and conduction layers, respectively. We plot $M^\lambda(\boldsymbol{q})$ of the triple-Q state for $J/t < 4$ and the ferromagnetic state for $J/t \geqslant 4$.

$M_\alpha^s(\boldsymbol{q})$ and $M_\alpha^c(\boldsymbol{q})$ are small and they have finite values in the thermodynamic limit. These results suggest that the ground state for $J/t = 3$ is the triple-Q state.

Figure 4(b) shows J dependence of $M_\alpha^\lambda(\boldsymbol{Q})$. In the gray region, we plot $M_\alpha^\lambda(\boldsymbol{q})$ of the triple-Q state for simplicity. For $J/t < 4$, $M_\alpha^\lambda(\boldsymbol{Q})$ for $\alpha = x, y$ and z is finite at $\boldsymbol{Q} = (\pi, 0)$, $(0, \pi)$ and (π, π), respectively. This suggests that the triple-Q state is indeed the ground state in the range of J/t. The magnetic ordered moments of the localized spins decrease by increasing J/t due to the Kondo screening. The reduction of the magnetic moment, $\Delta M = 0.5 - |M^s|$, is about 0.1 for $J/t = 3$. This small reduction may be related to the fact that the triple-Q state has the additional Z_2 symmetry breaking of the spin scalar chirality as discussed in the linear-spin wave analysis [36].

Before the transition to the ferromagnetic phase ($J/t \leqslant 4$), the magnetic ordered moments on the conduction layer show the nonmonotonic J/t dependence. This behavior can be attributed to the dual nature of the Kondo coupling: It can induce both the magnetic ordered states and the singlet state. Similar

nonmonotonic behavior is also found in the Kondo lattice model on a square lattice at half filling [50].

Around $J/t \sim 4$, we find that there is the first transition from the triple-Q state to the ferromagnetic state. Since $|M^c|$ is much smaller than $|M^s|$, the net magnetization of ferromagnetic state is finite. For $J/t > 4$, the J dependence of the magnetization is small. This result implies that nearly all the conduction electrons contribute to the formation of the Kondo singlets. The reduction of the magnetization of the localized spins ΔM is about 0.2.

B. Many-body Chern number

The triple-Q magnetic insulator is expected to have finite Chern number [26,28]. To calculate the many-body Chern number, we evaluate expectation values of Resta's polarization operator with the flux insertion [42,43,48]. The procedure is summarized as follows: we first introduce a flux in the hopping terms along the x direction as $t_{ij} \to t_{ij} \exp(-i\theta_x(x_{ic} - x_{jc})/L)$ defined in Eq. (1) and obtain the ground state of the Hamiltonian with the flux. The normalized ground-state wave functions is described as $|\bar{\psi}(\theta_x)\rangle$. Then, we calculate the expectation value of the polarization operator along the y direction, which is defined as

$$P_y(\theta_x) = \langle \bar{\psi}(\theta_x)| \exp\left(\frac{2\pi i}{L}\sum_j n_{jc}y_{jc}\right)|\bar{\psi}(\theta_x)\rangle. \quad (6)$$

The many-body Chern number $\mathcal{C}$ is obtained as the slope of the argument of $P_y(\theta_x)$, namely,

$$\varphi_y(\theta_x) = \arg[P_y(\theta_x)], \quad (7)$$

$$\mathcal{C} = \left.\frac{\partial \varphi_y(\theta_x)}{\partial \theta_x}\right|_{\theta_x \to 0}. \quad (8)$$

We note that the expectation value of the polarization operator in Eq. (6) can be easily calculated by the VMC method since it only includes the real-space diagonal operator $n_{jc}y_{jc}$. We also note that it is pointed out that the thermodynamic limit of Resta's formula may need special care in more than two dimensions [51].

Figure 5 shows θ_x dependence of $\varphi_y(\theta_x)$ in the triple-Q state for $J/t = 3$. In this state, we find that $\varphi(\theta_x)$ linearly increases as a function of θ_x and its slope is evaluated as 1.007(74) for $L = 14$ by the linear regression. This result indicates that the triple-Q state is the many-body Chern insulator with $\mathcal{C} = 1$. For comparison, we also calculate $\varphi(\theta_x)$ for a nonmagnetic Kondo insulator in the square lattice at half filling [50,52], which is expected to be a topologically trivial insulator. As a result, we find that the slope of $\varphi(\theta_x)$ is almost zero in the nonmagnetic Kondo insulator, which indicates that this state is a trivial insulator.

IV. SUMMARY AND DISCUSSION

In summary, we have performed the mVMC calculations for the Kondo lattice model on the triangular lattice at quarter filling. We find that the triple-Q magnetic ordered phase becomes the ground state in the intermediate coupling region. By explicitly calculating the many-body Chern number, we
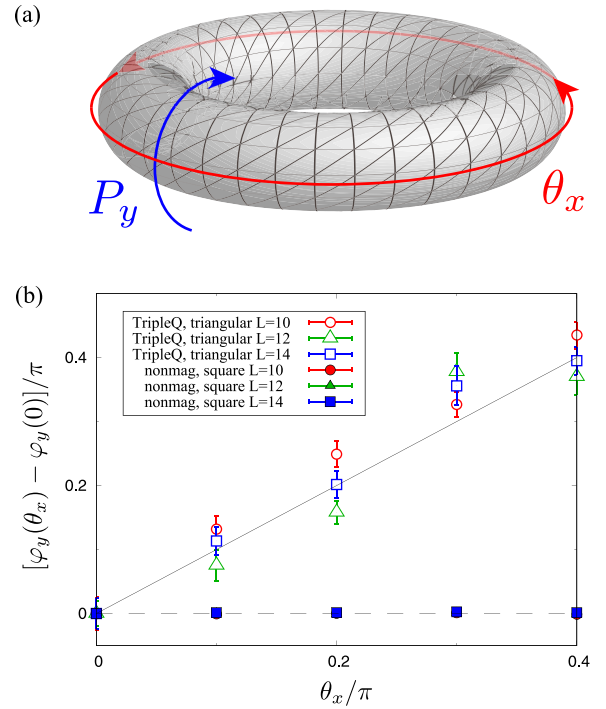

FIG. 5. (a) Schematic figure of the polarization operator along the y direction (P_y) and the flux θ_x along the x direction on the torus. (b) Flux dependence of the argument of the polarization $\varphi_y(\theta_x)$ in the triple-Q state at $J/t = 3$ (open symbols). For reference, we calculate $\varphi_y(\theta_x)$ for the nonmagnetic Kondo insulator in the Kondo lattice model on the square lattice at half filling and $J/t = 3$ (closed symbols). See Eq. (1) for the definition of the Kondo lattice model. Note that the variational parameters in the pair product part f_{IJ} are treated as complex numbers in these calculations. As a guide for the eye, we plot the thin line for $\varphi_y(\theta_x) = \theta_x + \varphi_y(0)$ and the dashed line for $\varphi_y(\theta_x) = \varphi_y(0)$.

show that the triple-Q state is indeed magnetic Chern insulators with $\mathcal{C} = 1$.

Here, we discuss the stability of the triple-Q state in the Kondo lattice model. In the classical limit and the spin wave analysis [28,29,36], the triple-Q magnetic order becomes the ground states for $2.8 < J/t < 18$, which is quite robust compared with our results [53]. Our results indicate the quantum effects significantly destabilize the triple-Q state. This destabilization may be attributed to the absence of the effective biquadratic term in the Kondo lattice model. In the classical limit at quarter filling, it has been shown that the effective positive biquadratic terms derived by a perturbation theory play an important role in inducing the noncoplanar spin configuration [29]. It is also discussed that the positive biquadratic term is significant in understanding the triple-Q state in itinerant magnets [54–56]. However, this term does not exist in the Kondo lattice model with spin $1/2$ since it is equivalent to the ferromagnetic Heisenberg interaction with an additional constant term. This ferromagnetic Heisenberg interaction stabilizes the collinear ferromagnetic state and does not induce the noncoplanar triple-Q state. Nevertheless, we show that the triple-Q state still survives in the Kondo lattice model. This indicates that itinerant magnets including spin $1/2$ localized spins can have the triple-Q state. Furthermore, the triple-Q

state with a large charge gap is expected to be more thermally stable than other Chern insulators found in previous studies, most of which are realized below about 20 K [56–58]. Thus our results are expected to stimulate the exploration of the triple-Q state at high temperatures and the resultant magnetic Chern insulator in a wide range of correlated electron systems. One of the possible candidates is a van der Walls heterostructure recently found in the experiment [56,59].

Lastly, we discuss how to further stabilize the triple-Q state. One promising way to stabilize the triple-Q state is adding the onsite Coulomb interaction to the conduction layer. In the triangular Hubbard model at quarter filling, the mean-field results suggest that the noncoplanar state becomes the ground state in the intermediate coupling region [60]. The recent mean-field study also shows that skyrmion crystals with triple-Q spin structures emerge around quarter filling [61]. Analysis of such an extended Kondo lattice model on the

triangular lattice is an intriguing issue but is also left for future study.

[1] J. Kondo, Resistance minimum in dilute magnetic alloys, Prog. Theor. Phys. **32**, 37 (1964).

[2] H. Tsunetsugu, M. Sigrist, and K. Ueda, The ground-state phase diagram of the one-dimensional Kondo lattice model, Rev. Mod. Phys. **69**, 809 (1997).

[3] G. R. Stewart, Non-Fermi-liquid behavior in d- and f-electron metals, Rev. Mod. Phys. **73**, 797 (2001).

[4] H. v. Löhneysen, A. Rosch, M. Vojta, and P. Wölfle, Fermi-liquid instabilities at magnetic quantum phase transitions, Rev. Mod. Phys. **79**, 1015 (2007).

[5] P. Gegenwart, Q. Si, and F. Steglich, Quantum criticality in heavy-fermion metals, Nat. Phys. **4**, 186 (2008).

[6] Q. Si and F. Steglich, Heavy fermions and quantum phase transitions, Science **329**, 1161 (2010).

[7] M. A. Ruderman and C. Kittel, Indirect exchange coupling of nuclear magnetic moments by conduction electrons, Phys. Rev. **96**, 99 (1954).

[8] T. Kasuya, A theory of metallic ferro- and antiferromagnetism on Zener's model, Prog. Theor. Phys. **16**, 45 (1956).

[9] K. Yosida, Magnetic properties of Cu-Mn alloys, Phys. Rev. **106**, 893 (1957).

[10] S. Doniach, The Kondo lattice and weak antiferromagnetism, Physica B+C **91**, 231 (1977).

[11] C. Zener, Interaction between the d-shells in the transition metals. II. Ferromagnetic compounds of manganese with perovskite structure, Phys. Rev. **82**, 403 (1951).

[12] P. G. de Gennes, Effects of double exchange in magnetic crystals, Phys. Rev. **118**, 141 (1960).

[13] K. Kubo and N. Ohata, A quantum theory of double exchange. I, J. Phys. Soc. Jpn. **33**, 21 (1972).

[14] J. Otsuki, H. Kusunose, and Y. Kuramoto, The Kondo lattice model in infinite dimensions: II. Static susceptibilies and phase diagram, J. Phys. Soc. Jpn. **78**, 034719 (2009).

[15] R. Peters, S. Hoshino, N. Kawakami, J. Otsuki, and Y. Kuramoto, Charge order in Kondo lattice systems, Phys. Rev. B **87**, 165133 (2013).

[16] T. Misawa, J. Yoshitake, and Y. Motome, Charge order in a two-dimensional Kondo lattice model, Phys. Rev. Lett. **110**, 246401 (2013).

[17] Y. Motome, K. Nakamikawa, Y. Yamaji, and M. Udagawa, Partial Kondo screening in frustrated Kondo lattice systems, Phys. Rev. Lett. **105**, 036403 (2010).

[18] T. Sato, F. F. Assaad, and T. Grover, Quantum Monte Carlo simulation of frustrated Kondo lattice models, Phys. Rev. Lett. **120**, 107201 (2018).

[19] T. H. Hsieh, Y.-M. Lu, and A. W. W. Ludwig, Topological bootstrap: Fractionalization from Kondo coupling, Sci. Adv. **3**, e1700729 (2017).

[20] O. Bodensiek, R. Žitko, M. Vojta, M. Jarrell, and T. Pruschke, Unconventional superconductivity from local spin fluctuations in the Kondo lattice, Phys. Rev. Lett. **110**, 146406 (2013).

[21] J. Otsuki, Competing d-wave and p-wave spin-singlet superconductivities in the two-dimensional Kondo lattice, Phys. Rev. Lett. **115**, 036404 (2015).

[22] W. Choi, P. W. Klein, A. Rosch, and Y. B. Kim, Topological superconductivity in the Kondo-Kitaev model, Phys. Rev. B **98**, 155123 (2018).

[23] J. Bedow, E. Mascot, T. Posske, G. S. Uhrig, R. Wiesendanger, S. Rachel, and D. K. Morr, Topological superconductivity induced by a triple-**q** magnetic structure, Phys. Rev. B **102**, 180504(R) (2020).

[24] Y.-Y. Chang, K. V. Nguyen, K.-L. Chen, Y.-W. Lu, C.-Y. Mou, and C.-H. Chung, Topological Kondo superconductors, arXiv:2301.00538.

[25] K. Ohgushi, S. Murakami, and N. Nagaosa, Spin anisotropy and quantum Hall effect in the kagomé lattice: Chiral spin state based on a ferromagnet, Phys. Rev. B **62**, R6065 (2000).

[26] I. Martin and C. D. Batista, Itinerant electron-driven chiral magnetic ordering and spontaneous quantum Hall effect in triangular lattice models, Phys. Rev. Lett. **101**, 156402 (2008).

[27] S. Kumar and J. van den Brink, Frustration-induced insulating chiral spin state in itinerant triangular-lattice magnets, Phys. Rev. Lett. **105**, 216405 (2010).

[28] Y. Akagi and Y. Motome, Spin chirality ordering and anomalous Hall effect in the ferromagnetic Kondo lattice model on a triangular lattice, J. Phys. Soc. Jpn. **79**, 083711 (2010).

[29] Y. Akagi, M. Udagawa, and Y. Motome, Hidden multiple-spin interactions as an origin of spin scalar chiral order in frustrated Kondo lattice models, Phys. Rev. Lett. **108**, 096401 (2012).

[30] C.-Z. Chang, J. Zhang, X. Feng, J. Shen, Z. Zhang, M. Guo, K. Li, Y. Ou, P. Wei, L.-L. Wang *et al.*, Experimental observation of the quantum anomalous Hall effect in a magnetic topological insulator, Science **340**, 167 (2013).

[31] Y. Tokura, K. Yasuda, and A. Tsukazaki, Magnetic topological insulators, Nat. Rev. Phys. **1**, 126 (2019).

[32] B. A. Bernevig, C. Felser, and H. Beidenkopf, Progress and prospects in magnetic topological materials, Nature (London) **603**, 41 (2022).

[33] F. D. M. Haldane, Model for a quantum Hall effect without Landau levels: Condensed-matter realization of the "parity anomaly", Phys. Rev. Lett. **61**, 2015 (1988).

[34] C.-X. Liu, X.-L. Qi, X. Dai, Z. Fang, and S.-C. Zhang, Quantum anomalous Hall effect in $Hg_{1-y}Mn_yTe$ quantum wells, Phys. Rev. Lett. **101**, 146802 (2008).

[35] C.-X. Liu, S.-C. Zhang, and X.-L. Qi, The quantum anomalous Hall effect: Theory and experiment, Annu. Rev. Condens. Matter Phys. **7**, 301 (2016).

[36] Y. Akagi, M. Udagawa, and Y. Motome, Effect of quantum spin fluctuation on scalar chiral ordering in the Kondo lattice model on a triangular lattice, J. Phys. Soc. Jpn. **82**, 123709 (2013).

[37] T. Fukui, Y. Hatsugai, and H. Suzuki, Chern numbers in discretized brillouin zone: Efficient method of computing (spin) Hall conductances, J. Phys. Soc. Jpn. **74**, 1674 (2005).

[38] S. Coh and D. Vanderbilt, Electric polarization in a Chern insulator, Phys. Rev. Lett. **102**, 107603 (2009).

[39] Q. Niu, D. J. Thouless, and Y.-S. Wu, Quantized Hall conductance as a topological invariant, Phys. Rev. B **31**, 3372 (1985).

[40] K. Shiozaki, H. Shapourian, K. Gomi, and S. Ryu, Many-body topological invariants for fermionic short-range entangled topological phases protected by antiunitary symmetries, Phys. Rev. B **98**, 035151 (2018).

[41] K. Kudo, H. Watanabe, T. Kariyado, and Y. Hatsugai, Many-body Chern number without integration, Phys. Rev. Lett. **122**, 146601 (2019).

[42] B. Kang, W. Lee, and G. Y. Cho, Many-body invariants for Chern and Chiral hinge insulators, Phys. Rev. Lett. **126**, 016402 (2021).

[43] H. Dehghani, Z.-P. Cian, M. Hafezi, and M. Barkeshli, Extraction of the many-body Chern number from a single wave function, Phys. Rev. B **103**, 075102 (2021).

[44] D. Tahara and M. Imada, Variational Monte Carlo method combined with quantum-number projection and multi-variable optimization, J. Phys. Soc. Jpn. **77**, 114701 (2008).

[45] M. Kurita, Y. Yamaji, S. Morita, and M. Imada, Variational Monte Carlo method in the presence of spin-orbit interaction and its application to Kitaev and Kitaev-Heisenberg models, Phys. Rev. B **92**, 035122 (2015).

[46] T. Misawa, S. Morita, K. Yoshimi, M. Kawamura, Y. Motoyama, K. Ido, T. Ohgoe, M. Imada, and T. Kato, mVMC—Open-source software for many-variable variational Monte Carlo method, Comput. Phys. Commun. **235**, 447 (2019).

[47] F. Becca and S. Sorella, *Quantum Monte Carlo Approaches for Correlated Systems* (Cambridge University Press, Cambridge, 2017).

[48] R. Resta, Quantum-mechanical position operator in extended systems, Phys. Rev. Lett. **80**, 1800 (1998).

[49] S. Sorella, Generalized Lanczos algorithm for variational quantum Monte Carlo, Phys. Rev. B **64**, 024512 (2001).

[50] S. Capponi and F. F. Assaad, Spin and charge dynamics of the ferromagnetic and antiferromagnetic two-dimensional half-filled Kondo lattice model, Phys. Rev. B **63**, 155114 (2001).

[51] H. Watanabe and M. Oshikawa, Inequivalent Berry phases for the bulk polarization, Phys. Rev. X **8**, 021065 (2018).

[52] F. F. Assaad, Quantum Monte Carlo simulations of the Half-filled two-dimensional Kondo lattice model, Phys. Rev. Lett. **83**, 796 (1999).

[53] Note that the exchange interactions in the classical Kondo-lattice model J_{cl} is four times smaller than the exchange interactions defined in Eq. (1), i.e., $J_{cl} = J/4$.

[54] R. Takagi, J. S. White, S. Hayami, R. Arita, D. Honecker, H. M. Rønnow, Y. Tokura, and S. Seki, Multiple-q noncollinear magnetism in an itinerant hexagonal magnet, Sci. Adv. **4**, eaau3402 (2018).

[55] P. Park, W. Cho, C. Kim, Y. An, Y.-G. Kang, M. Avdeev, R. Sibille, K. Iida, R. Kajimoto, K. H. Lee *et al.*, Tetrahedral triple-Q magnetic ordering and large spontaneous Hall conductivity in the metallic triangular antiferromagnet $Co_{1/3}TaS_2$, Nat. Commun. **14**, 8346 (2023).

[56] H. Takagi, R. Takagi, S. Minami, T. Nomoto, K. Ohishi, M.-T. Suzuki, Y. Yanagi, M. Hirayama, N. Khanh, K. Karube *et al.*, Spontaneous topological Hall effect induced by non-coplanar antiferromagnetic order in intercalated van der Waals materials, Nat. Phys. **19**, 961 (2023).

[57] Y. Deng, Y. Yu, M. Z. Shi, Z. Guo, Z. Xu, J. Wang, X. H. Chen, and Y. Zhang, Quantum anomalous Hall effect in intrinsic magnetic topological insulator $MnBi_2Te_4$, Science **367**, 895 (2020).

[58] Y. Okazaki, T. Oe, M. Kawamura, R. Yoshimi, S. Nakamura, S. Takada, M. Mogi, K. S. Takahashi, A. Tsukazaki, M. Kawasaki *et al.*, Quantum anomalous Hall effect with a permanent magnet defines a quantum resistance standard, Nat. Phys. **18**, 25 (2022).

[59] V. Vaño, M. Amini, S. C. Ganguli, G. Chen, J. L. Lado, S. Kezilebieke, and P. Liljeroth, Artificial heavy fermions in a van der Waals heterostructure, Nature (London) **599**, 582 (2021).

[60] T. Li, Metal-insulator transition in quarter-filled Hubbard model on triangular lattice and its implication for the physics of $Na_{0.5}CoO_2$, arXiv:1001.0620.

[61] K. Kobayashi and S. Hayami, Skyrmion and vortex crystals in the Hubbard model, Phys. Rev. B **106**, L140406 (2022).

[62] K. Momma and F. Izumi, *VESTA 3* for three-dimensional visualization of crystal, volumetric and morphology data, J. Appl. Crystallogr. **44**, 1272 (2011).